Electronic Supplementary Material (ESI) for RSC Advances.

Supporting Information for

Aromatic Copolyesters with Enhanced Crystallizability and Mechanical Property by Adding the Renewable Nipagin-based Composition

Keling Hu,[†] Guolin Wu*[†] and Jianbiao Ma*[‡]

[†] Key Laboratory of Functional Polymer Materials of MOE, Institute of Polymer Chemistry, Nankai University, Tianjin 300071, P. R. China

[‡] School of Chemistry and Chemical Engineering, Tianjin University of Technology, Tianjin 300191, P. R. China

Correspondence to: guolinwu@hotmail.com

1. Experimental Section

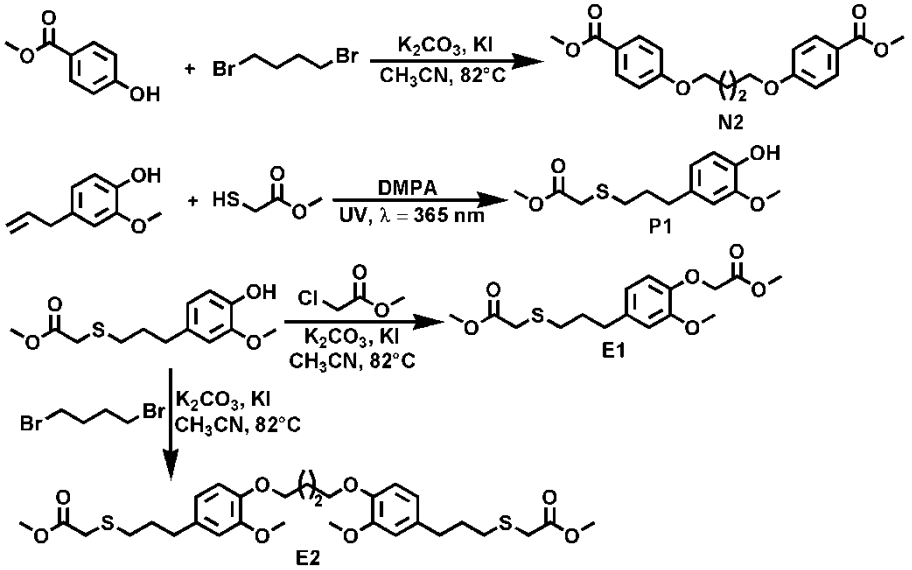

Scheme S1 Synthetic routes for the preparation of the nipagin and eugenol-based dimethyl esters.

Synthesis of Nipagin and Eugenol-based Dimethyl Esters

Synthesis of 4,4'-[1,4-Butanediyl-Bisoxy] Bis-1,1'-Dimethyl Benzoate (N2).

Nipagin (12.90 g, 84 mmol), 1,4-dibromobutane (8.64 g, 40 mmol), anhydrous K_2CO_3 (11.70 g, 84 mmol), KI (0.32 g, 2 mmol) and 300 mL anhydrous CH_3CN were added into a 500 mL three-necked round bottom flask equipped with a magnetic stirrer (Scheme S1). Subsequently, the mixture was refluxed at 82 °C for 24 hours under nitrogen atmosphere. The progress of the reaction was monitored by TLC. After completion of the reaction, the suspension was cooled to room temperature. A modified method was used for the post-process. First, the cooled suspension was immediately concentrated under vacuum to obtain a yellow solid. This solid was washed with distilled water to remove the inorganic salts. Then the insoluble solid was filtered off and extracted from chloroform thrice. Finally, the combined chloroform extracts were concentrated under vacuum to afford a white solid, which was subjected to recrystallization twice from methanol to obtain 13.18 g **N2** as a white solid. Yield 92%; mp 146-148 °C.

^{1}H NMR (400 MHz, $CDCl_3$): δ 8.02-7.95 (m, 4H; Ar-*H*), 6.95-6.86 (m, 4H; Ar-*H*), 4.15-4.03 (m, 4H; ArO-CH_2-), 3.88 (s, 6H; ArCO-CH_3), 2.06-1.95 (m, 4H; ArOCH$_2$-CH_2-) ppm; ^{13}C NMR (100.6 MHz, $CDCl_3$): δ 166.84 (Ar-*C*O-), 162.74 (Ar-*C*), 131.62 (Ar-*C*), 122.63 (Ar-*C*), 114.09 (Ar-*C*), 67.61 (ArO-*C*H$_2$-), 51.84 (ArCOO-*C*H$_3$), 25.88 (ArOCH$_2$-*C*H$_2$-) ppm (Fig. S1-S2); HRMS (ESI) m/z: $[M+H]^+$ calcd for $C_{20}H_{23}O_6$: 359.1495; found: 359.1492. $[M+Na]^+$ calcd for $C_{20}H_{22}NaO_6$: 381.1314; found: 381.1311.

Synthesis of 2-Methoxy-4-[3-(2-Methoxy-2-Oxoethyl)]thiopropyl Phenol (P1).

Eugenol (13.24 g, 80 mmol), methyl thioglycolate (10.28g, 96 mmol), and 2,2-dimethoxy-2-phenylacetophenone (DMPA, 0.1028 g, 0.4 mmol) as the photoinitiator, were added into a 50 mL quartz tube and thoroughly mixed into a homogeneous solution (Scheme S1). Then the reaction mixture was irradiated with four 6W ultraviolet lamps (λ = 365 nm). The reaction was detected by TLC until eugenol completely disappearing. The crude product was directly purified by column chromatography ($V_{petroleum\ ether}$: $V_{ethyl\ acetate}$ = 5 : 1) to afford 10.24 g **P1** as a light yellow oil. Yield 95%; bp 183-185 ℃ (5 mmHg).

^{1}H NMR (400 MHz, $CDCl_3$): δ 6.83–6.65 (m, 3H; Ar-*H*), 5.53 (s, 1H; Ar-O*H*), 3.86 (s, 3H; ArO-C*H*$_3$), 3.71 (s, 3H; -COO-C*H*$_3$), 3.22 (s, 2H; -S-C*H*$_2$-CO-), 2.61-2.66 (m, 4H; -S-C*H*$_2$-CH$_2$-C*H*$_2$-), 1.93-1.85 (q, *J* = 7.3 Hz, 2H; -SCH$_2$-C*H*$_2$-) ppm; ^{13}C NMR (100.6 MHz, $CDCl_3$): δ 171.07 (-SCH$_2$-*C*O-), 146.61 (Ar-*C*), 143.94 (Ar-*C*), 133.20 (Ar-*C*), 121.03 (Ar-*C*), 114.46 (Ar-*C*), 111.28 (Ar-*C*), 55.92 (ArO-*C*H$_3$), 52.32(-COO-*C*H$_3$), 34.27 (-S-*C*H$_2$-CO-), 33.43 (Ar-*C*H$_2$-), 32.05 (-S-*C*H$_2$-CH$_2$-), 30.79 (-SCH$_2$-*C*H$_2$-) ppm (Fig. S3-S4); HRMS (ESI) m/z: $[M-H]^-$ calcd for $C_{13}H_{17}O_4S$: 269.0848; found: 269.0852.

Synthesis of Methyl 2-{2-Methoxy-4-[3-(2-Methoxy-2-Oxoethyl)]thiopropyl}phenoxy Acetate (E1).

Precursor **P1** (10.80 g, 40 mmol), methyl chloroacetate (10.64 g, 80 mmol), anhydrous K_2CO_3 (11.04 g, 80 mmol), KI (0.33 g, 2 mmol) and 200 mL anhydrous CH_3CN were added into a 500 mL three-necked round bottom flask equipped with a magnetic stirrer (Scheme S1). The reaction mixture was refluxed at 82 ℃ for 6 hours under nitrogen atmosphere. The progress of the reaction was monitored by TLC. After finish of the reaction, the suspension was cooled to room temperature, white solid was filtered off. The filtrate was concentrated under vacuum to obtain a viscous oil, which was dissolved in 350 mL dichloromethane and successively washed by distilled water (2 × 120 mL) and saturated NaCl solution (2 × 120 mL). The organic phase was dried over anhydrous magnesium sulphate and concentrated under vacuum. The resulting residue was purified by column chromatography ($V_{petroleum\ ether}$: $V_{ethyl\ acetate}$ = 3 : 1) to afford 11.84 g **E1** as a light yellow viscous oil. Yield 88%; bp 196-197 ℃ (5 mmHg).

^{1}H NMR (400 MHz, $CDCl_3$): δ 6.78-6.66 (m, 3H; Ar-*H*), 4.66 (s, 2H; ArO-C*H*$_2$-CO-), 3.87 (s, 3H; ArO-C*H*$_3$), 3.78 (s, 3H; ArOCH$_2$COO-C*H*$_3$), 3.71 (s, 3H; -SCH$_2$COO-C*H*$_3$), 3.22 (s, 2H; -S-C*H*$_2$-CO-), 2.68-2.61 (m, 4H; -S-C*H*$_2$-CH$_2$-C*H*$_2$-), 1.94-1.86 (q, *J* = 7.4 Hz, 2H; -SCH$_2$-C*H*$_2$-CH$_2$-) ppm; ^{13}C NMR (100.6 MHz, $CDCl_3$): δ 170.85 (-SCH$_2$-*C*O-), 169.54 (ArOCH$_2$-*C*O-), 149.58 (Ar-*C*), 145.52 (Ar-*C*), 135.82 (Ar-*C*), 120.28 (Ar-*C*), 114.74 (Ar-*C*), 112.57 (Ar-*C*), 66.67 (ArO-*C*H$_2$-CO-), 55.85 (ArO-*C*H$_3$), 52.23 (-CH$_2$COO-*C*H$_3$), 52.01 (-SCH$_2$COO-*C*H$_3$), 34.16 (-S-*C*H$_2$-CO-), 33.35 (-SCH$_2$CH$_2$-*C*H$_2$-), 31.97 (-SCH$_2$-*C*H$_2$-CH$_2$-), 30.50 (-S-*C*H$_2$-CH$_2$CH$_2$-) ppm (Fig. S5-S6); HRMS (ESI) m/z: $[M+Na]^+$ calcd for $C_{16}H_{23}O_6NaS$: 365.1035; found: 365.1035.

Synthesis of 1,4-Bis{2-Methoxy-4-[3-(2-Methoxy-2-Oxoethyl)]thiopropyl}phenoxy Butane (E2).

Precursor **P1** (22.68 g, 84 mmol), 1,4-dibromobutane (8.72 g, 40 mmol), anhydrous K_2CO_3 (12.12 g, 88 mmol), KI (0.33 g, 2 mmol) and 300 mL anhydrous CH_3CN were added into a 500 mL three-necked round bottom flask equipped with a magnetic stirrer (Scheme S1). The reaction mixture was refluxed at 82 ℃ for 48 hours under nitrogen atmosphere. The progress of the reaction was monitored by TLC. After finish of the reaction, the suspension was cooled to room temperature, white solid was filtered off. The filtrate was concentrated under vacuum to obtain a viscous oil, which was dissolved in 400 mL dichloromethane and successively washed by water (2 × 150 mL) and saturated NaCl solution (2 × 150 mL). The organic phase was dried over anhydrous magnesium sulphate and concentrated under vacuum. The resulting residue was directly purified by twice-recrystallization from methanol to afford 9.74 g **E2** as a white crystalline solid. Yield 86%; mp 78-79 ℃.

^{1}H NMR (400 MHz, $CDCl_3$): δ 6.82-6.67 (m, 3H; Ar-*H*), 4.06 (m, 4H; ArO-C*H*$_2$-), 3.84 (s, 6H; ArO-C*H*$_3$), 3.72 (s, 6H; -SCH$_2$COO-C*H*$_3$), 3.22 (s, 4H; -S-C*H*$_2$-CO-), 2.67-2.62 (m, 8H; -S-C*H*$_2$-CH$_2$-), 2.01 (m, 4H; -OCH$_2$-C*H*$_2$-), 1.94-1.87 (q, *J* = 7.2 Hz, 4H; -SCH$_2$-C*H*$_2$-)

ppm; ^{13}C NMR (100.6 MHz, $CDCl_3$): δ 170.96 (-SCH_2-*C*O-), 149.47 (Ar-*C*), 146.83 (Ar-*C*), 134.14 (Ar-*C*), 120.41 (Ar-*C*), 113.48 (Ar-*C*), 112.45 (Ar-*C*), 68.88 (ArO-*C*H_2-), 56.00 (ArO-*C*H_3), 52.33 (-SCH_2COO-*C*H_3), 34.23 (-S-*C*H_2-CO-), 33.48 (-SCH_2CH_2-*C*H_2-), 32.10 (-S-*C*H_2-CH_2-), 30.68 (-SCH_2-*C*H_2-), 26.10 (ArOCH_2-*C*H_2-) ppm (Fig. S5, Fig. S7); HRMS (ESI) m/z: $[M+Na]^+$ calcd for $C_{30}H_{42}O_8NaS_2$: 617.2219; found: 617.2218.

2. Characterization Section

Table S1 Powder X-ray diffraction data of **PDN2$_{1-x}$E1$_x$** and **PDN2$_{1-x}$E2$_x$** copolyesters

	X-ray diffraction data					
Copolyester	2θ (°)[a]					X_c[b]
PDN2	14.56 w	16.22 w	17.74 m	19.24 m	24.08 s	0.75
PDN2$_{90\%}$E1$_{10\%}$	14.56 w	16.22 w	17.74 m	19.24 m	24.08 s	0.68
PDN2$_{90\%}$E2$_{10\%}$	14.56 w	16.22 w	17.74 m	19.24 m	24.08 s	0.64
PDN2$_{80\%}$E1$_{20\%}$	14.56 w	16.22 w	17.74 m	19.24 m	24.08 s	0.62
PDN2$_{80\%}$E2$_{20\%}$	14.56 w	16.22 w	17.74 m	19.24 m	24.08 s	0.60
PDN2$_{70\%}$E1$_{30\%}$	14.56 w	16.22 w	17.74 m	19.24 m	24.08 s	0.54
PDN2$_{70\%}$E2$_{30\%}$	14.56 w	16.22 w	17.74 m	19.24 m	24.08 s	0.52
PDN2$_{60\%}$E1$_{40\%}$	14.56 w	16.22 w	17.74 w	19.24 w	24.08 s	0.45
PDN2$_{60\%}$E2$_{40\%}$	14.56 w	16.22 w	17.74 w	19.24 w	24.08 s	0.44
PDN2$_{50\%}$E1$_{50\%}$	14.56 w	16.22 w	17.74 w	19.24 w	24.08 s	0.38
PDN2$_{50\%}$E2$_{50\%}$	14.56 w	16.22 w	17.74 w	19.24 w	24.08 s	0.36

[a] The diffraction angles measured in powder diffraction patterns for samples coming directly from synthesis. Intensities visually estimated as follows: m, medium; s, strong; w, weak. [b] Crystallinity index calculated as the quotient between crystalline area and total area. Crystalline and amorphous areas in the X-ray diffraction pattern were quantified using PeakFit v4.12 software.

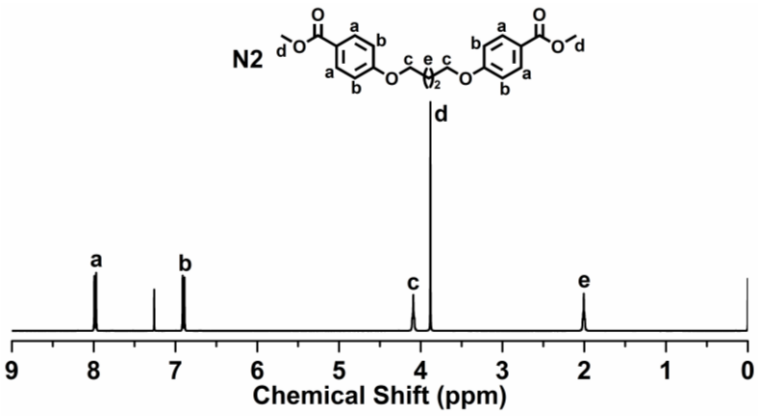

Fig. S1 ^{1}H NMR spectrum of **N2**.

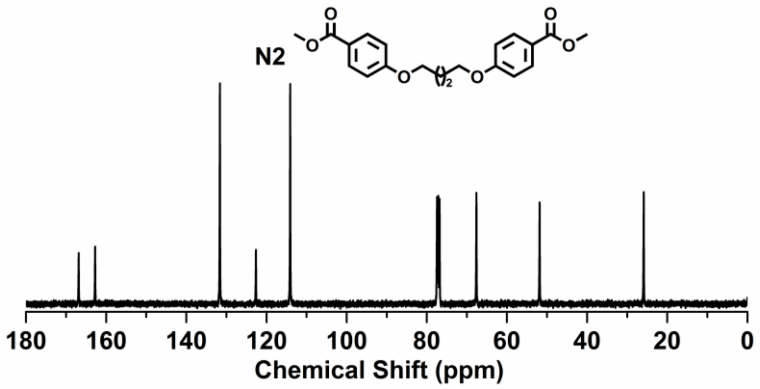

Fig. S2 ^{13}C NMR spectrum of **N2**.

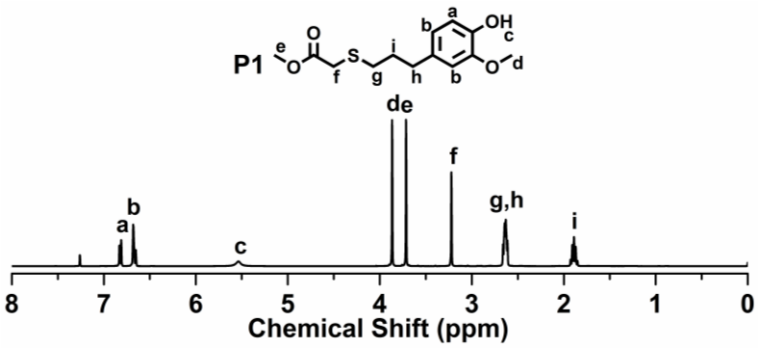

Fig. S3 ^{1}H NMR spectrum of **P1**.

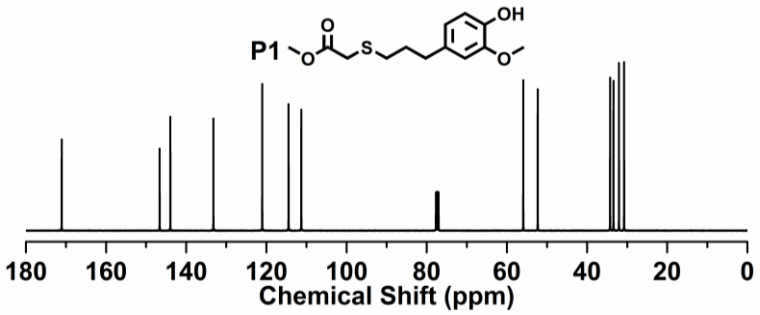

Fig. S4 ^{13}C NMR spectrum of **P1**.

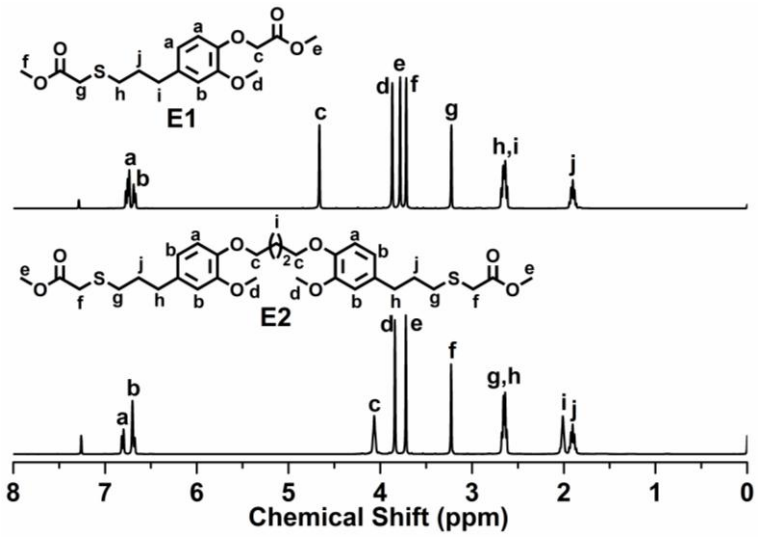

Fig. S5 ^{1}H NMR spectra of **E1** and **E2**.

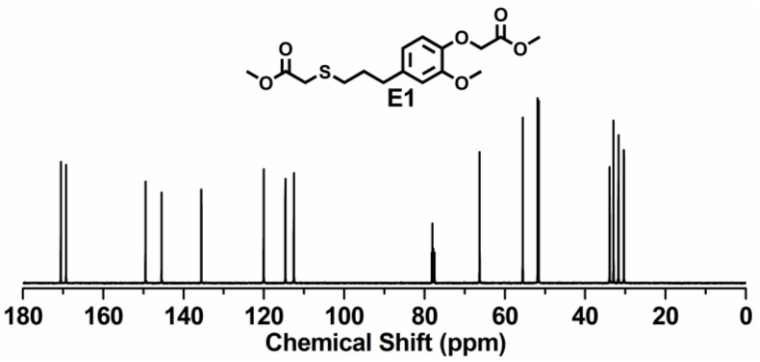

Fig. S6 ^{13}C NMR spectrum of **E1**.

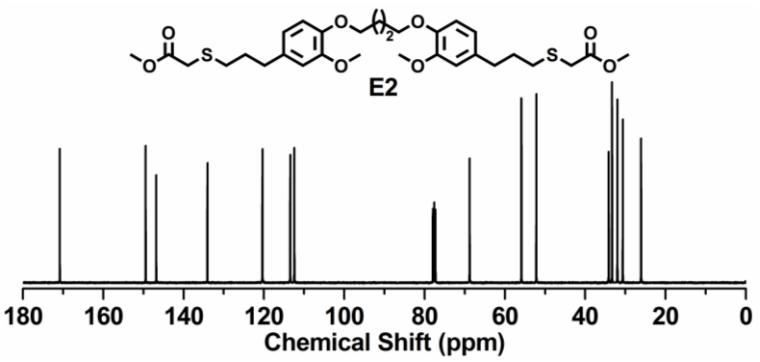

Fig. S7 ^{13}C NMR spectrum of **E2**.

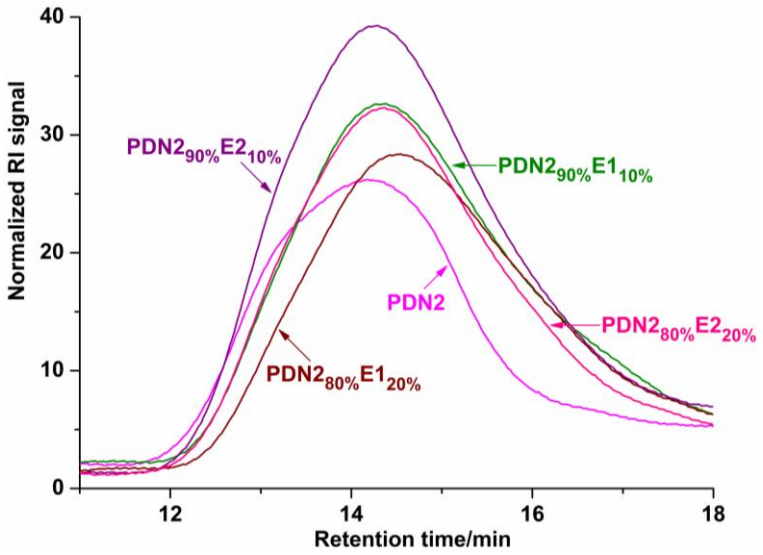

Fig. S8 SEC traces of the corresponding copolyesters carried out in $CHCl_3$.

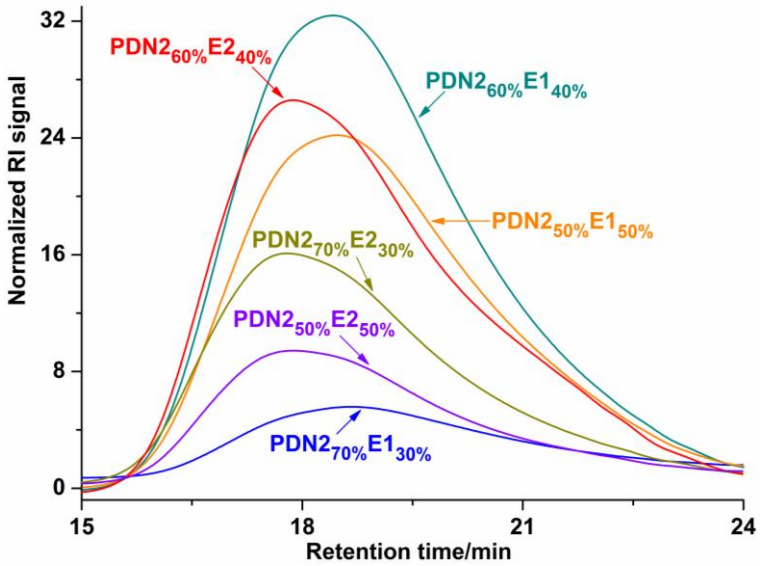

Fig. S9 SEC traces of the corresponding copolyesters carried out in THF.

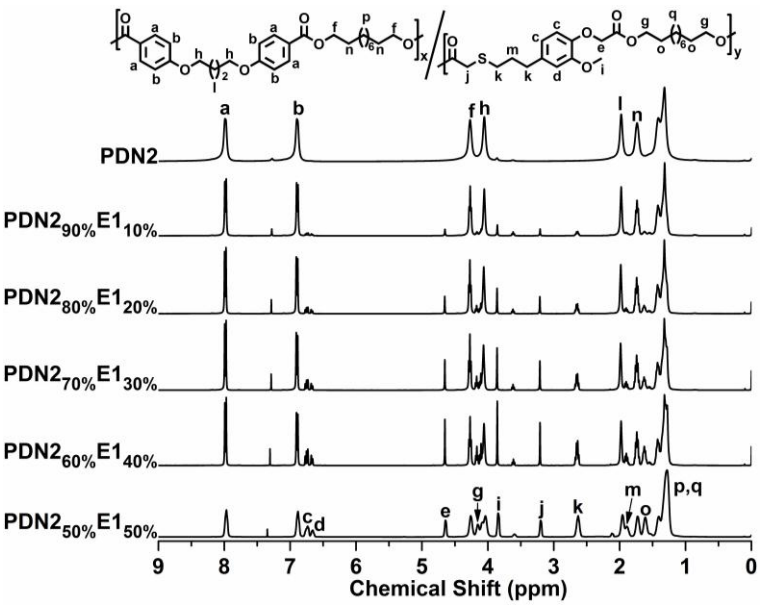

Fig. S10 ^{1}H NMR spectra of **PDN2$_{1-x}$E1$_x$** copolyesters.

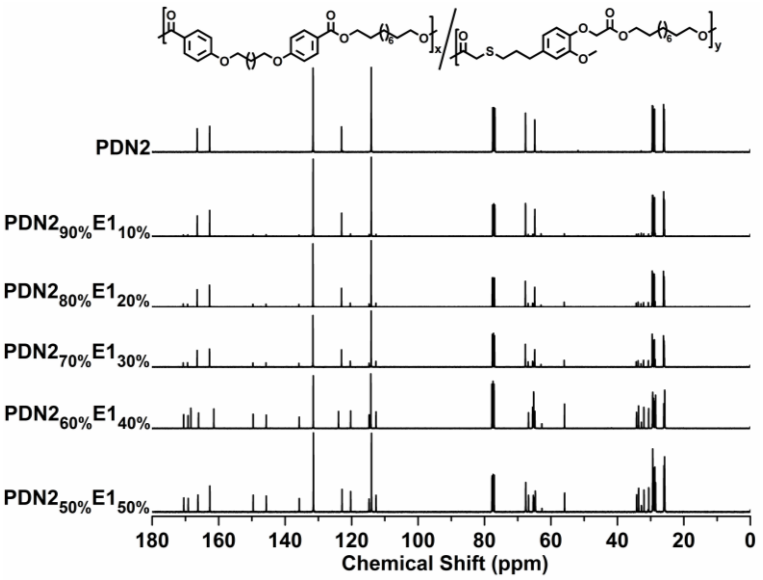

Fig. S11 ^{13}C NMR spectra of **PDN2$_{1-x}$E1$_x$** copolyesters.

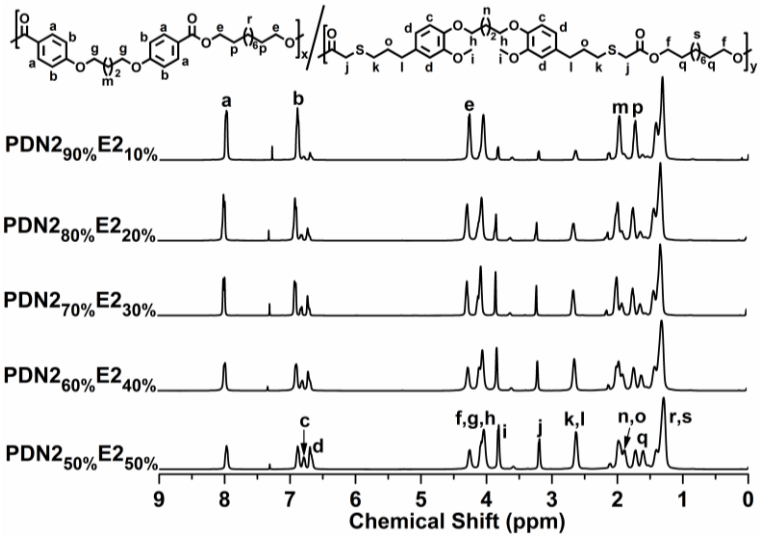

Fig. S12 ^{1}H NMR spectra of **PDN2$_{1-x}$E2$_{x}$** copolyesters.

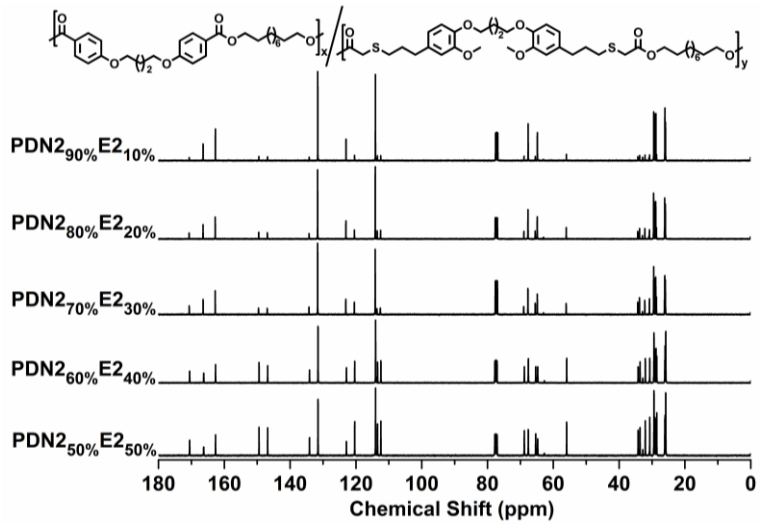

Fig. S13 ^{13}C NMR spectra of **PDN2$_{1-x}$E2$_{x}$** copolyesters.

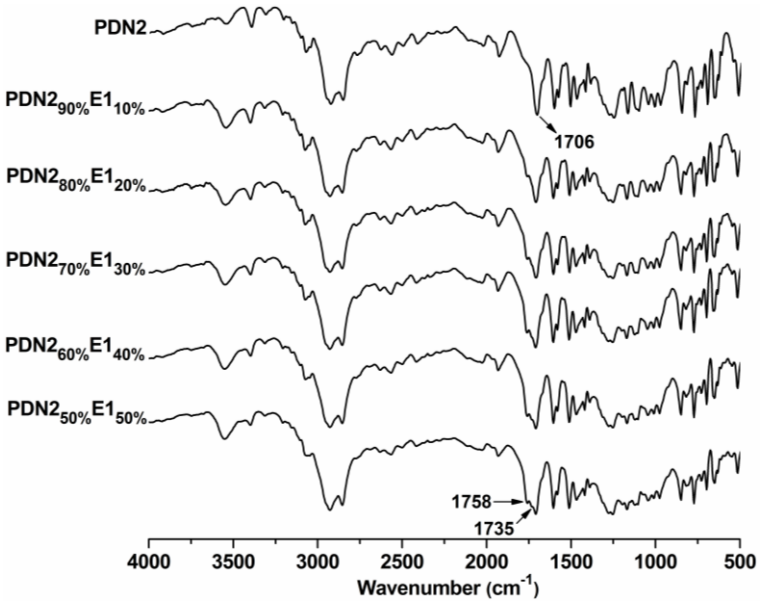

Fig. S14 FTIR spectra of **PDN2$_{1-x}$E1$_x$** copolyesters.

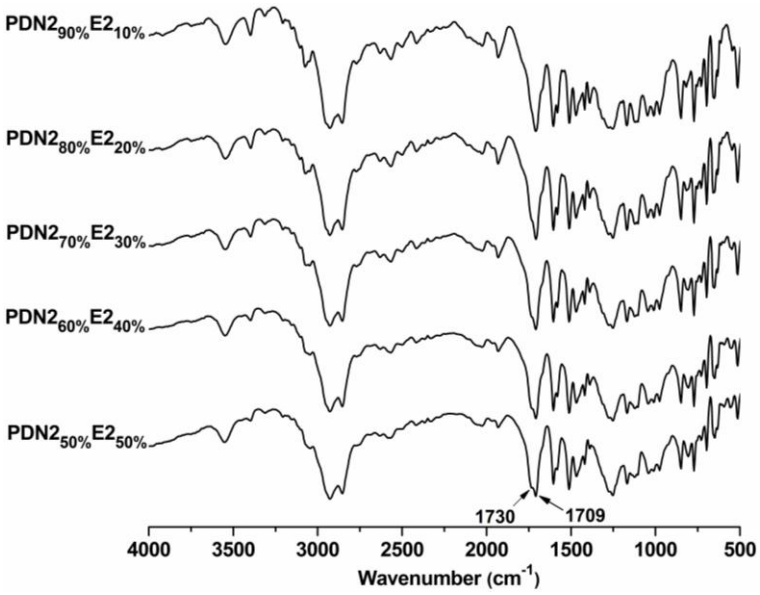

Fig. S15 FTIR spectra of **PDN2$_{1-x}$E2$_x$** copolyesters.

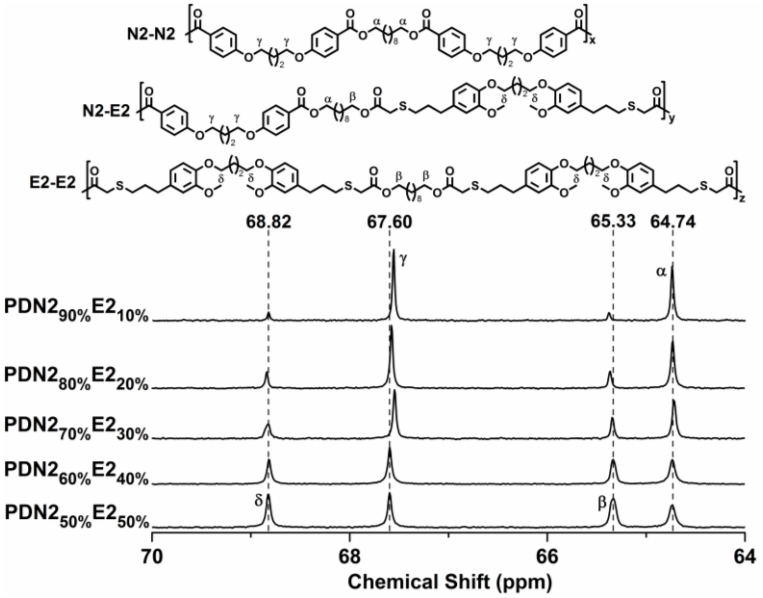

Fig. S16 The splitting situations of the methylenes adjacent to the hydroxy-oxygens with the indications of the dyads to which they are assigned in **PDN2$_{1-x}$E2$_x$** copolyesters.

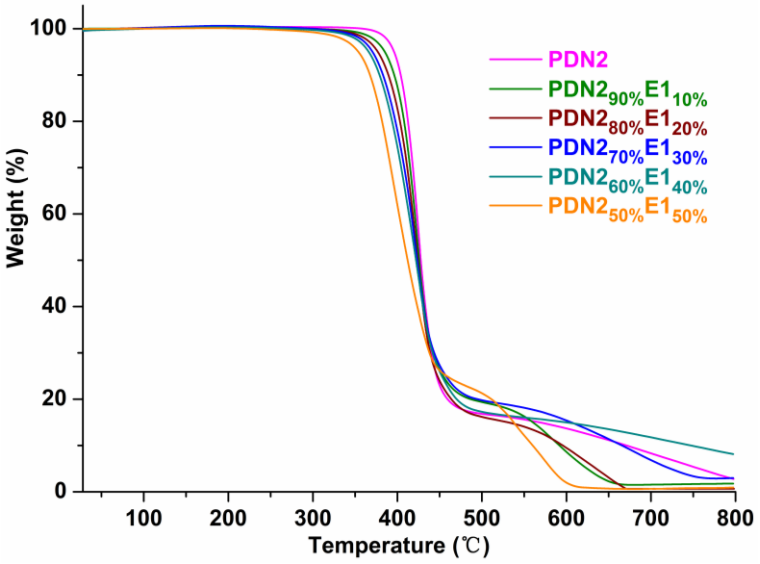

Fig. S17 TGA curves of **PDN2$_{1-x}$E1$_x$** copolyesters.

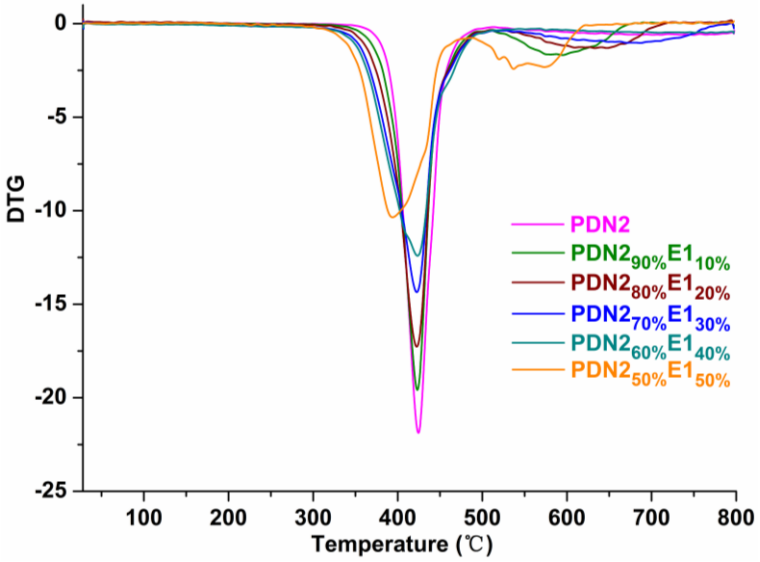

Fig. S18 TGA derivative curves of **PDN2$_{1-x}$E1$_x$** copolyesters.

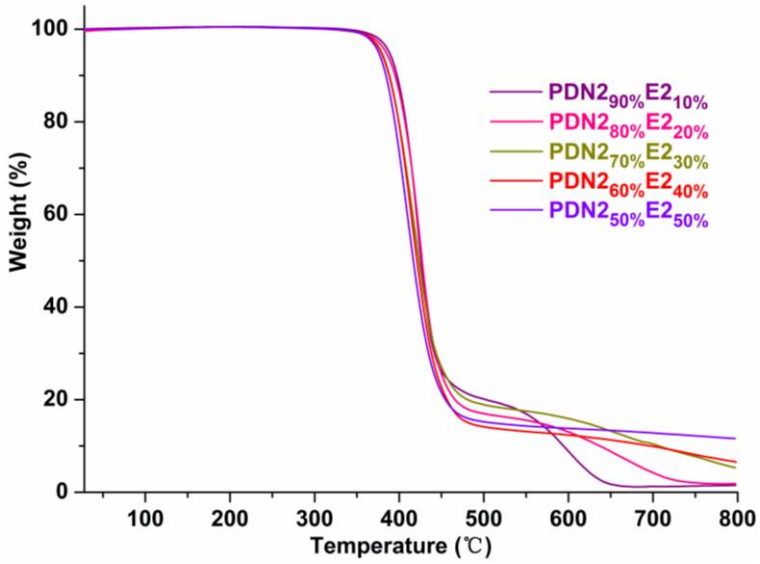

Fig. S19 TGA curves of **PDN2$_{1-x}$E2$_x$** copolyesters.

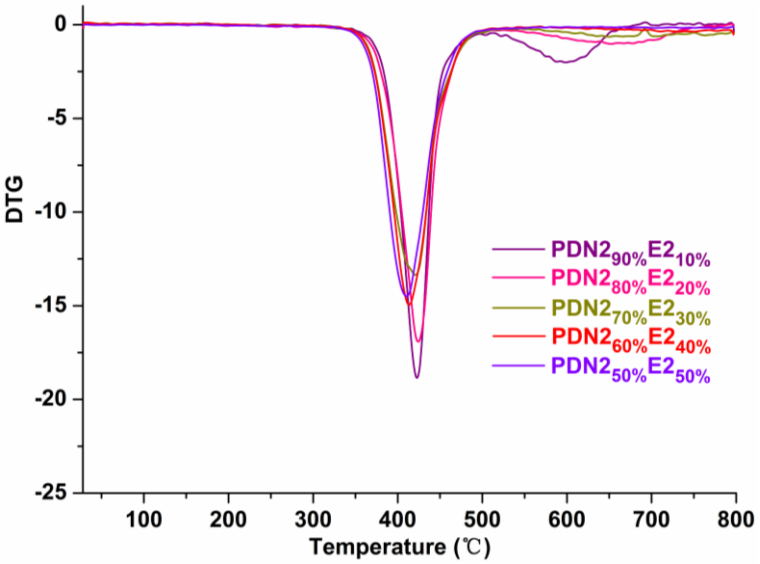

Fig. S20 TGA derivative curves of **PDN2$_{1-x}$E2$_x$** copolyesters.

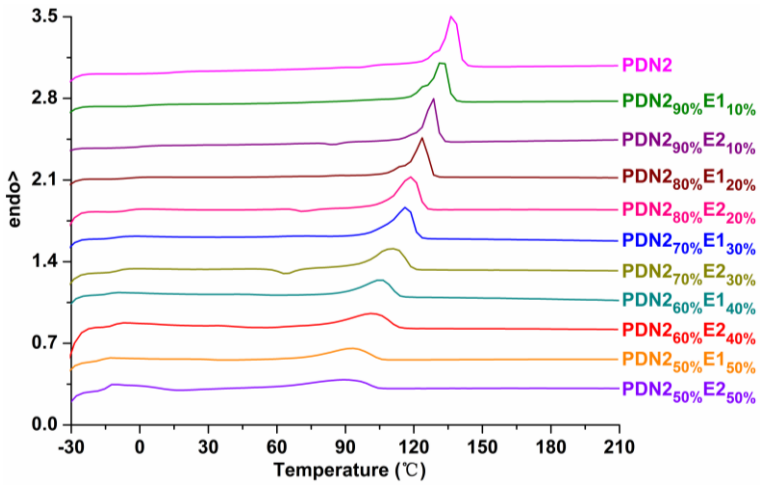

Fig. S21 Second heating DSC curves of the copolyesters coming from samples after precipitation from methanol carried out from -30 to 210 ℃ at a heating / cooling rate of 10 ℃ min^{-1}.

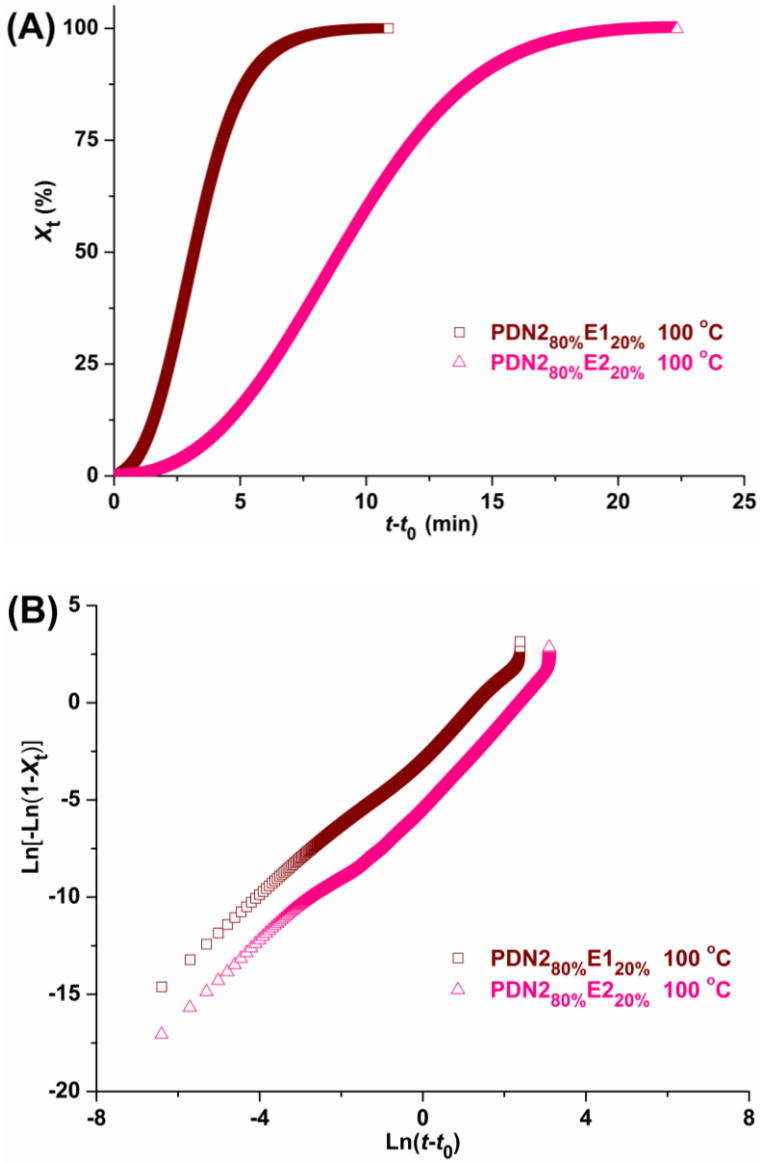

Fig. S22 Isothermal crystallization of **PDN2$_{80\%}$E1$_{20\%}$** and **PDN2$_{80\%}$E2$_{20\%}$** at the indicated temperature. Relative crystallinity versus time plots (A) and Ln[-Ln(1-X_t)] versus Ln(t-t_0) plots (B).

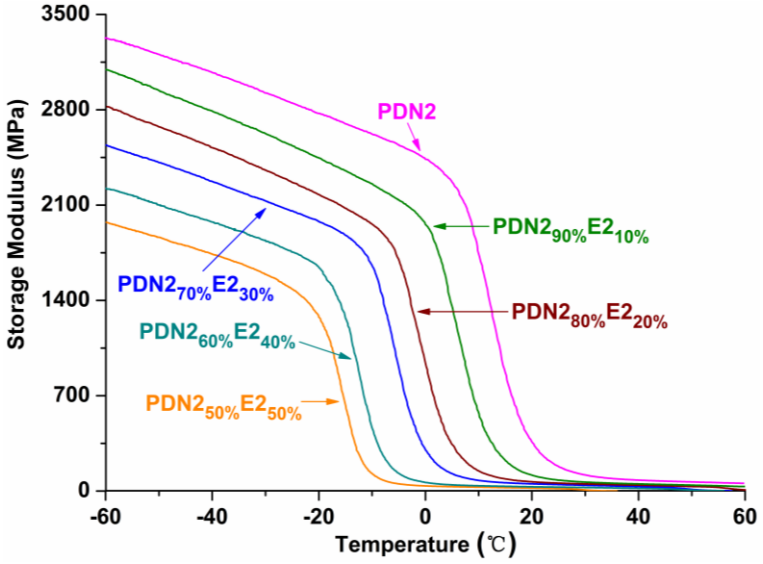

Fig. S23 Storage mudulus as a function of temperature for **PDN2$_{1-x}$E2$_x$** copolyesters.

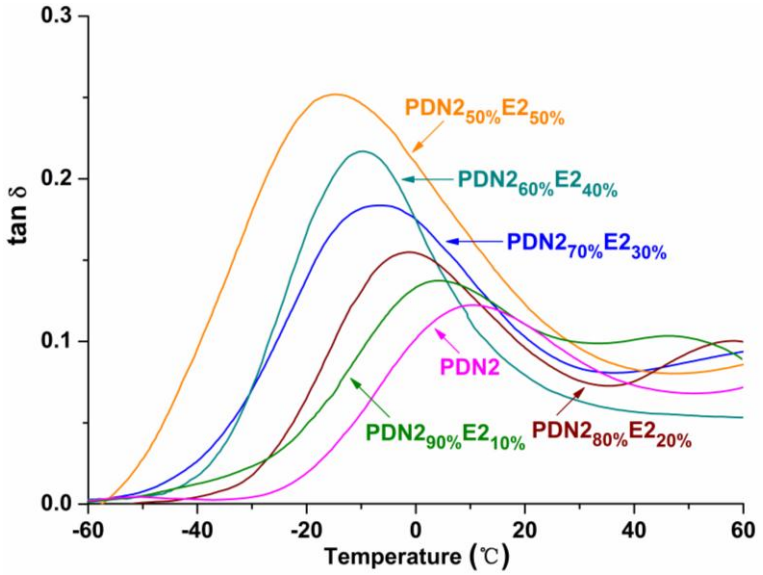

Fig. S24 Tan δ as a function of temperature for **PDN2$_{1-x}$E2$_x$** copolyesters.